Chapter 7

Wavelength-Division-Multiplexed Coherent Systems

7.1 Crosstalk Issues

7.2 Cross-Phase Modulation Induced Nonlinear Phase Noise

In this section, the error probability is derived analytically for differential phase-shift keying (DPSK) signals contaminated by both self- and cross-phase modulation (SPM and XPM) induced nonlinear phase noise. XPM-induced nonlinear phase noise is modeled as Gaussian distributed phase noise. When fiber dispersion is compensated perfectly in each fiber span, XPM-induced nonlinear phase is summed coherently span after span and is the dominant nonlinear phase noise for typical wavelength-division-multiplexed (WDM) DPSK systems. For systems without or with XPM-suppressed dispersion compensation, SPM-induced nonlinear phase noise is usually the dominant nonlinear phase noise. With longer walk-off length, for the same mean nonlinear phase shift, 10-Gb/s systems are more sensitive to XPM-induced nonlinear phase noise than 40-Gb/s systems.

7.2.1 Nonlinear Phase Noise Variance due to Cross-Phase modulation

This section derives the ratio of the variance of nonlinear phase noise induced by XPM to that by SPM. The variance is first derived for the two-channel pump-probe model and later extended to multi-span WDM systems.

Pump-probe model

For the simplest model of having two WDM channel, the overall nonlinear phase shift to the first channel is equal to

$$\phi_{\mathrm{NL}} = \gamma \int_0^L \left[|E_1(z)|^2 + 2|E_2(z)|^2 \right] \mathrm{d}z \tag{7.1}$$

where E_1 and E_2 are the electric field of the first and second channel, respectively. In Eq. (7.1), the first term of the right-hand-size is from self-phase modulation (SPM) and have been considered in Chapters 5, 6 and the second term is from cross-phase modulation (XPM) that will be considered in this Chapter. If both the first and second channel propagates in the same speed in the fiber, the contribution from XPM is the same as that from SPM. However, with channel walk-off, we now face a different problem.

Based on the pump-probe model of (Chiang et al., 1994, 1996, Ho et al., 1999, Leibrich et al., 2002), the phase modulation of channel 1 (probe) induced by channel 2 (pump) is

$$\phi_{1,\mathrm{XPM}}(L, t) = 2\gamma \int_0^L P_2(0, t + d_{12} z) e^{-\alpha z} \mathrm{d}z. \tag{7.2}$$

where $P_2(z,t)$ is the power of channel 2 as a function of position z and time t, γ is the nonlinear coupling coefficient, α is fiber attenuation coefficient, L is the fiber length, $d_{12} \approx D\Delta\lambda$ is the relative walk-off between two channels with wavelength separation of $\Delta\lambda$, and D is the dispersion coefficient.

By taking the Fourier transform of the autocorrelation function, when the power spectral density of $P_2(0,t)$ is $\Phi_{P_2}(f)$, the power spectral density of $\phi_{1,\mathrm{XPM}}(L,t)$ is

$$\Phi_{\phi_1}(f) = \Phi_{P_2}(f)|H_{12}(f)|^2, \tag{7.3}$$

where $H_{12}(f) = 2\gamma \int_0^L e^{-\alpha z + j2\pi f d_{12} z} \mathrm{d}z$ or (Chiang et al., 1994, 1996)

$$H_{12}(f) = 2\gamma \frac{1 - e^{-\alpha L + j2\pi f d_{12} L}}{\alpha - j2\pi f d_{12}}. \tag{7.4}$$

At the DPSK receiver, after the asymmetric Mach-Zehnder interferometer (Gnauck et al., 2002, 2003, Ho, 2003d), the differential nonlinear phase noise of $\Delta\phi_{1,\mathrm{XPM}}(L,t) = \phi_{1,\mathrm{XPM}}(L,t) - \phi_{1,\mathrm{XPM}}(L,t-T)$ adds to the differential phase of the signal, where T is the symbol interval. Similar to (Kim, 2003), the power spectral density of $\Delta\phi_{1,\mathrm{XPM}}(L,t)$ is

$$\Phi_{\Delta\phi_1}(f) = 4\Phi_{P_2}(f)|H_{12}(f)|^2 \sin^2(\pi f T). \tag{7.5}$$

When the pump (channel 2) has amplifier noises, $P_2(0,t) = |E_2 + N_2|^2$ where E_2 and N_2 are the electric fields for signal and noise, respectively. In the power of $P_2(0,t) = |E_2|^2 + E_2 \cdot N_2^* + E_2^* \cdot N_2 + |N_2|^2$, the dc-term of $|E_2|^2$ gives no nonlinear phase noise but a constant phase shift, the signal-noise beating of $E_2 \cdot N_2^* + E_2^* \cdot N_2$ gives a noise spectral density of $2|E_2|^2 S_{\mathrm{sp}}$, the noise-noise beating of $|N_2|^2$ gives a noise spectral density of $2S_{\mathrm{sp}}^2 \Delta\nu_{\mathrm{opt}}$, where S_{sp} is the spectral density of the amplifier noise and $\Delta\nu_{\mathrm{opt}}$ is the optical bandwidth of the amplifier noise. The optical signal-to-noise ratio (SNR) over an optical bandwidth of $\Delta\nu_{\mathrm{opt}}$ is $|E_2|^2/(2S_{\mathrm{sp}}\Delta\nu_{\mathrm{opt}})$. For a launched power of P_0 and a single optical amplifier with a noise variance of $S_{\mathrm{sp},1}$, we get $\Phi_{P_2}(f) = n_0 = 2P_0 S_{\mathrm{sp},1} + 2S_{\mathrm{sp},1}^2 \Delta\nu_{\mathrm{opt}}$. The phase variance as a function of frequency separation is

$$\sigma_{\mathrm{XPM},0}^2(\Delta\lambda) = 4n_0 \int_{-1/T}^{1/T} |H_{12}(f)|^2 \sin^2(\pi f T)\, \mathrm{d}f, \tag{7.6}$$

where the integration is reduced from $\pm\infty$ to $\pm 1/T$ by taking into account only the phase noise over a bandwidth confined within the bit-rate. The dependence of the variance of Eq. (7.6) on $\Delta\lambda$ is originated from the dependence of $H_{12}(f)$ of Eq. (7.4) on $\Delta\lambda$.

For SPM-induced nonlinear phase noise, using Eq. (7.6), we get $\sigma_{\mathrm{SPM}}^2 = \frac{1}{4}\sigma_{\mathrm{XPM},0}^2(0) = 4n_0\gamma^2 L_{\mathrm{eff}}^2/T$, where $L_{\mathrm{eff}} = (1 - e^{-\alpha L})/\alpha$ is the effective length per span. The factor of $\frac{1}{4}$ is because phase shift induced by XPM is twice larger than that induced by SPM for the same intensity. For a long fiber span with $L \gg 1/\alpha$ and large walk-off coefficient of d_{12}, using (Gradshteyn and Ryzhik, 1980, §3.824), we get

$$\begin{aligned} \frac{\sigma_{\mathrm{XPM},0}^2(\Delta\lambda)}{\sigma_{\mathrm{SPM}}^2} &= 8\alpha^2 T \int_0^{1/T} \frac{\sin^2(\pi f T)}{\alpha^2 + (2\pi f d_{12})^2} \mathrm{d}f \\ &\approx 8\alpha^2 T \int_0^{\infty} \frac{\sin^2(\pi f T)}{\alpha^2 + (2\pi f d_{12})^2} \mathrm{d}f \\ &= \alpha L_W (1 - e^{-\alpha L_W}), \end{aligned} \tag{7.7}$$

where $L_W = T/|d_{12}|$ is the walk-off length that is the distance for two aligned pump and probe pulses of length T becomes completely walk-off (Ho, 2000). Like that for stimulated Raman scattering (Ho, 2000), even without approximation, the variances of XPM-induced nonlinear phase noise depends on the walk-off length of L_W only.

Multi-span WDM systems

For a $(2M+1)$-channel WDM system, for the worse case of the center channel, in the first span, the nonlinear phase noise variance per span is equal to

$$\sigma^2_{\mathrm{XPM},1} = 2\sum_{k=1}^{M} \sigma^2_{\mathrm{XPM},0}(k\Delta\lambda), \tag{7.8}$$

where, using the same symbol as the above pump-probe model, $\Delta\lambda$ is the wavelength separation between adjacent channels. For a short walk-off length of L_W per channel separation of $\Delta\lambda$, a wavelength separation of $k\Delta\lambda$ gives a XPM-induced nonlinear phase noise variance of about a factor of $1/k^2$ smaller than that for a wavelength separation of $\Delta\lambda$. For large number of channels, using the relationship of $\sum_{k=1}^{\infty}\frac{1}{k^2} = \frac{\pi^2}{6}$ (Gradshteyn and Ryzhik, 1980, §0.233), we get

$$\lim_{M\to\infty} \frac{\sigma^2_{\mathrm{XPM},1}}{\sigma^2_{\mathrm{SPM}}} \approx \frac{\pi^2}{3}\alpha L_W(1-e^{-\alpha L_W}). \tag{7.9}$$

For a system with N fiber spans, the variance of the overall XPM-induced nonlinear phase noise depends on the method of dispersion compensation. Similar to Eq. (7.5), the power spectrum density of XPM-induced nonlinear phase noise after K fiber spans is (Chiang et al., 1996)

$$\begin{aligned}\Phi_{K,\Delta\phi_1}(f) &= 4\Phi_{P_2}(f)|H_{12}(f)|^2\sin^2(\pi f T)\\ &\quad\times\left|\frac{\sin[K\pi f(1-\kappa)d_{12}L]}{\sin[\pi f(1-\kappa)d_{12}L]}\right|^2,\end{aligned} \tag{7.10}$$

where κ is the fraction of dispersion compensation, i.e., $\kappa = 1$ and $\kappa = 0$ for perfect and without dispersion compensation, respectively.

In the worst case of perfect dispersion compensation with $\kappa = 1$ such that all channels are well-aligned when launch to each fiber span, the variance of Eq. (7.6) is increased by a factor of K^2 after K fiber spans. With perfect dispersion compensation, the variance of the overall XPM-induced nonlinear phase noise for an N-span fiber system is

$$\sigma^2_{\mathrm{XPM,max}} = N^2\sigma^2_{\mathrm{XPM},1} + (N-1)^2\sigma^2_{\mathrm{XPM},2} + \cdots + \sigma^2_{\mathrm{XPM},N}, \tag{7.11}$$

where the first term of $\sigma^2_{\mathrm{XPM},1}$ is the nonlinear phase noise induced from the amplifier noise from the first span, the second term is the nonlinear phase noise induced from the amplifier noise from the second span, and so on. Because of perfect dispersion compensation, the same noise from the first span is perfectly (or coherently) added N times into the overall nonlinear phase noise. The noise from the second span $\sigma^2_{\mathrm{XPM},2}$ adds into the overall nonlinear phase noise $N-1$ times. With the assumption that all spans have the same configuration, $\sigma^2_{\mathrm{XPM},1} = \sigma^2_{\mathrm{XPM},2} = \cdots = \sigma^2_{\mathrm{XPM},N}$. The maximum nonlinear phase noise of Eq. (7.11) is

$$\sigma^2_{\mathrm{XPM,max}} = \frac{1}{6}N(N+1)(2N+1)\sigma^2_{\mathrm{XPM},1}. \tag{7.12}$$

For SPM-induced nonlinear phase noise, the amplifier noise from the first span is also perfectly aligned in all fiber spans afterward. The relationship between single- and multi-span phase noise variance is the same as that of Eq. (7.12). With perfect dispersion compensation, the ratio of the variance of XPM- to SPM-induced nonlinear phase noise is independent of the number of fiber spans in WDM systems. The ratio of Eq. (7.9) can be used to approximate the ratio of XPM- to SPM-induced nonlinear phase noise in the worst-case of perfect dispersion compensation.

When dispersion compensation is conducted channel-by-channel with XPM-suppression (Bellotti and Bigo, 2000, Bellotti et al., 2000), the factor of κ is the offset of pump and probe at the output of a fiber span with respect to the fiber walk-off. If $|\kappa| \gg 1$ such that the nonlinear phase noise induced to every fiber span is independent of each other, we get

$$\sigma^2_{\mathrm{XPM,ind}} = N\sigma^2_{\mathrm{XPM},1} + (N-1)\sigma^2_{\mathrm{XPM},2} + \cdots + \sigma^2_{\mathrm{XPM},N}, \tag{7.13}$$

or

$$\sigma^2_{\mathrm{XPM,ind}} = \frac{1}{2}N(N+1)\sigma^2_{\mathrm{XPM},1}, \tag{7.14}$$

and the ratio of

$$\frac{\sigma^2_{\mathrm{XPM,max}}}{\sigma^2_{\mathrm{XPM,ind}}} = \frac{1}{3}(2N+1). \tag{7.15}$$

In Eq. (7.13), the amplifier noise from the first span induces nonlinear phase noise in each fiber span. However, the nonlinear phase noises induced to the first and second span are from the amplifier noise in completely non-overlapped time interval and independent of each other. In an N-span system, the overall nonlinear phase noise is generated from $\frac{1}{2}N(N+1)$ "pieces" of independent amplifier noise. The variance of Eq. (7.13) is also valid when $L \gg L_W$ and $\kappa \neq 1$.

The last term of Eq. (7.10) due to multi-span effect of $\sin[K\pi f(1-\kappa)d_{12}L]/\sin[\pi f(1-\kappa)d_{12}L]$ has peak values of K or $-K$ when $f(1-\kappa)d_{12}L = k$, where k is positive or negative integer. The last term of Eq. (7.5) due to differential operation of $\sin^2(\pi f T)$ has notches at $f = k/T$. If the notches of $\sin^2(\pi f T)$ match to the peaks of $\sin[K\pi f(1-\kappa)d_{12}L]/\sin[\pi f(1-\kappa)d_{12}L]$, XPM-induced nonlinear phase noise is approximately minimized. If $L_W < L$, the dispersion compensation factor of

$$\kappa = 1 - \frac{L_W}{L} \tag{7.16}$$

approximately gives minimum XPM-induced nonlinear phase noise. With resonance effect (Nelson et al., 1999), certain combinations of walk-off length and dispersion compensation factor minimizes the variance of XPM-induced nonlinear phase noise. Numerical results show that the compensation factor of Eq. (7.16) approximately minimizes the variance of XPM-induced nonlinear phase noise.

Figure 7.1 shows the ratio of the standard deviation of XPM- to SPM-induced nonlinear phase noise as a function of the walk-off length L_W per channel separation $\Delta\lambda$. The ratio of $\sigma_{\mathrm{XPM,min}}/\sigma_{\mathrm{SPM}}$ shown as dotted lines is calculated numerically and uses the dispersion compensation factor of Eq. (7.16) for $L_W < L$ and $\kappa = 0$ for $L_W \geq L$. The fiber attenuation coefficient is $\alpha = 0.21$ dB/km. The fiber span length is $L = 80$ km. For the pump-probe model (labeled as "2" WDM channels), the approximation of Eq. (7.7) is valid for L_W less than 50 km.

For multi-channel WDM systems, in both the worst and independent cases, the approximation of Eq. (7.9) is valid for L_W less than 100 km and number of channels larger than 17. The approximation of Eq. (7.9) can be used to model typical WDM systems. For example, typical 10-Gb/s 50-GHz spacing system using non-zero dispersion-shifted fiber (NZDSF) with $D = 4$ ps/km/nm has a walk-off length of 62.5 km. Typical 40-Gb/s systems have a walk-off length of 7.8 km (100 GHz spacing and $D = 4$ ps/km/nm).

When the walk-off effect is weak with long walk-off length ($L_W > 100$ km), from the pump-probe model, the nonlinear phase noise standard deviation due to XPM approaches twice that due to SPM. With long walk-off length, nonlinear phase noise induced by XPM is much larger than that induced by SPM.

For a multi-span system, the variance of the SPM-induced nonlinear phase noise is equal to (Gordon and Mollenauer, 1990)

$$\sigma^2_{\mathrm{SPM}} \approx \frac{4 <\Phi_{\mathrm{NL}}>^2}{3\rho_s} \tag{7.17}$$

with the exact results given in (Ho and Kahn, 2004), where ρ_s is the SNR defined for optical matched filter and a single polarization (Ho, 2003a,b). The variance of Eq. (7.17) is twice that of (Gordon and Mollenauer, 1990, Ho and Kahn, 2004) for differential signal. Combined Eq. (7.17) with the ratio in Fig. 7.1, the variance of XPM-induced nonlinear phase noise σ^2_{XPM} can be calculated.

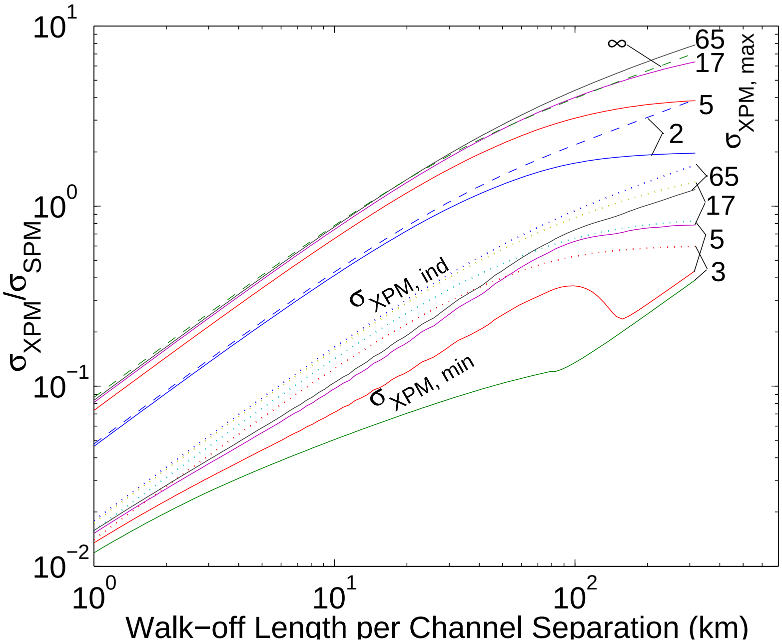

Figure 7.1: The ratio of $\sigma_{\mathrm{XPM}}/\sigma_{\mathrm{SPM}}$ as a function of walk-off length per channel separation. The dashed curves are the approximation of Eq. (7.7) and Eq. (7.9). The ratio for the worst-case of $\sigma_{\mathrm{XPM,max}}$ is independent of number of spans. The ratios for the typical cases of $\sigma_{\mathrm{XPM,ind}}$ and the minimum case of $\sigma_{\mathrm{XPM,min}}$ are for $N = 32$ fiber spans and show as dotted and solid lines, respectively. The label of each curve is the number of WDM channels.

7.2.2 Error Probability

From (Ho, 2003a), with only SPM-induced nonlinear phase noise, the error probability of a DPSK signal is

$$p_{e,\mathrm{SPM}} = \frac{1}{2} - \frac{\rho_s e^{-\rho_s}}{2} \sum_{k=0}^{\infty} \frac{(-1)^k}{2k+1} \left[I_k\!\left(\frac{\rho_s}{2}\right) + I_{k+1}\!\left(\frac{\rho_s}{2}\right)\right]^2 \times |\Psi_{\Phi_{\mathrm{NL}}}(2k+1)|^2. \tag{7.18}$$

where k is a summation index, $I_k(\cdot)$ is a kth-order modified Bessel function of the first kind, $\Psi_{\Phi_{\mathrm{NL}}}(\nu)$ is the characteristic function of SPM-induced nonlinear phase noise given by (Ho, 2003c). Simulation by error counting confirms the validity of the error probability of Eq. (7.18) (Ho, 2003a).

When independent phase noises from different sources are summed together, the coefficients of the Fourier series of the overall probability density function are the product of the corresponding Fourier coefficients of each individual component. If the XPM-induced nonlinear phase noise is Gaussian distributed, the error probability of the DPSK signal is

$$p_{e,\mathrm{XPM}} = \frac{1}{2} - \frac{\rho_s e^{-\rho_s}}{2} \sum_{k=0}^{\infty} \frac{(-1)^k}{2k+1} \left[I_k\!\left(\frac{\rho_s}{2}\right) + I_{k+1}\!\left(\frac{\rho_s}{2}\right)\right]^2 \times |\Psi_{\Phi_{\mathrm{NL}}}[(2k+1)j]|^2 \exp\left[-\frac{2k+1}{2}\sigma^2_{\mathrm{XPM}}\right]. \tag{7.19}$$

The formulas of Eq. (7.18) and Eq. (7.19) are similar to that with noisy reference (Jain, 1974), laser phase noise (Nicholson, 1984), phase error (Blachman, 1981), or laser phase noise together with phase error (Jacobsen and Garrett, 1987). The terms within the summation of Eq. (7.19) is the product of that due to SPM-induced nonlinear phase noise (Ho, 2003a) and laser phase noise (Nicholson, 1984).

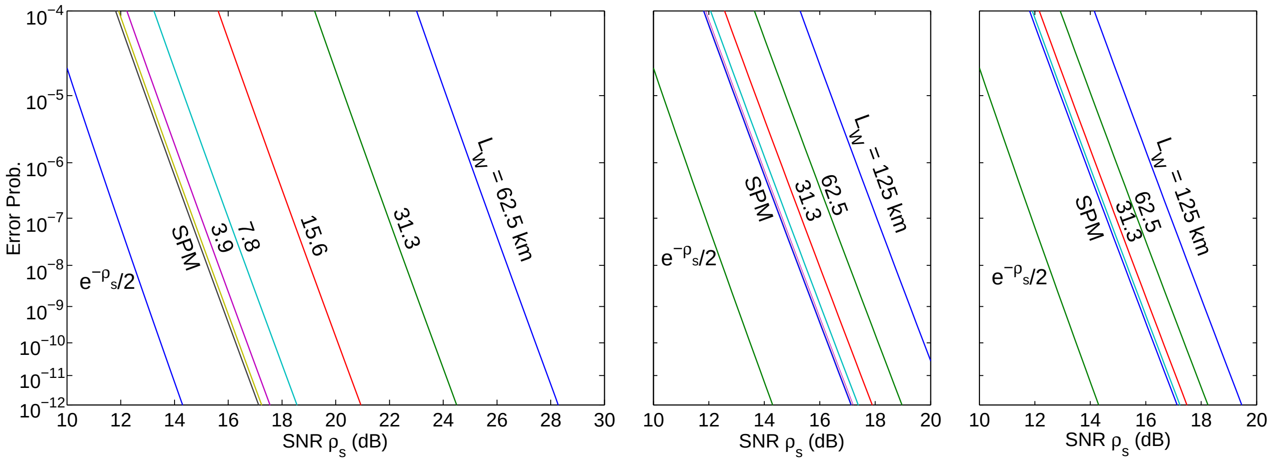

(a) $\sigma^2_{\rm XPM,max}$ (b) $\sigma^2_{\rm XPM,ind}$ (c) $\sigma^2_{\rm XPM,min}$

Figure 7.2: Error probability as a function of SNR for WDM DPSK systems with various dispersion compensation schemes, corresponding to (a) maximum, (b) independent, and (c) minimum variance of XPM-induced nonlinear phase noise.

Because XPM-induced nonlinear phase noise is generated by the interaction of many bits or WDM channels, the Gaussian approximation is valid from the central limit theorem (Papoulis, 1984). If the walk-off length of L_W is small, the nonlinear phase noise is induced by at least about $2 \times L_{\rm eff}/L_W$ independent bits from two adjacent channels (Forghieri et al., 1997, Ho, 2000). If the walk-off length is large, many adjacent channels induce more or less the same amount of nonlinear phase noise (Forghieri et al., 1995, 1997, Ho, 2000). In both cases, the central limit theorem leads to Gaussian distribution.

Figures 7.2 show the error probability of DPSK signal as a function of SNR ρ_s. The error probability is calculated by Eq. (7.18) and Eq. (7.19) for system with and without XPM-induced nonlinear phase noise, respectively. The system in Figs. 7.2 has $N = 32$ identical fiber spans, mean nonlinear phase shift of $<\Phi_{\rm NL}>= 1$ rad, and 65 WDM channels. The mean nonlinear phase shift of 1 rad is the same as the estimation from (Gordon and Mollenauer, 1990) and close to the optimal operating point from (Ho, 2003a). Taking into only SPM-induced nonlinear phase shift, the mean nonlinear phase shift can be calculated approximately from (Gordon and Mollenauer, 1990) and accurately from (Ho and Kahn, 2004). Figures 7.2 also plot the error probability of $\frac{1}{2}e^{-\rho_s}$ without nonlinear phase noise (Blachman, 1981, Ho, 2003a,b, Jain, 1974).

The walk-off length of Figs. 7.2 forms a geometric series and corresponds to typical 10- and 40-Gb/s systems in NZDSF and standard single-mode fiber (SSMF) with dispersion coefficients of $D = 4$ and 16 ps/km/nm, respectively. For example, the walk-off length $L_W = 7.8$ km is that of 10-Gb/s 100-GHz ($\Delta\lambda = 0.8$ nm) system in SSMF and 40-Gb/s 100-GHz system in NZDSF.

Figures 7.2(a), (b), and (c) are calculated using the XPM-induced nonlinear phase noise variances of $\sigma^2_{\rm XPM,max}$, $\sigma^2_{\rm XPM,ind}$, and $\sigma^2_{\rm XPM,min}$ in Eq. (7.19), respectively, corresponding to the worst, independent, and best case dispersion compensation, respectively. Comparing Figs. 7.2(b) and (c) with Fig. 7.2(a), DPSK system requires the reduction of XPM-induced nonlinear phase noise using, for example, XPM suppressor (Bellotti and Bigo, 2000, Bellotti et al., 2000) or optimal dispersion compensation factor of Eq. (7.16). With perfect dispersion compensation, XPM-induced cross-phase modulation is negligible if $L_W < 3.9$ km. Without dispersion compensation or with XPM suppressor, XPM-induced cross-phase modulation is negligible if $L_W < 15.8$ km.

Figures 7.3 show the SNR penalty for an error probability of 10^{-9} as a function of mean nonlinear phase shift of $<\Phi_{\rm NL}>$ for the same system as Figs. 7.2. Figures 7.3(a), (b), and (c) are calculated using the XPM-induced nonlinear phase noise variances of $\sigma^2_{\rm XPM,max}$, $\sigma^2_{\rm XPM,ind}$, and $\sigma^2_{\rm XPM,min}$ in Eq. (7.19), respectively, corresponding to the worst, independent, and best case dispersion compensation, respectively.

For the systems in Fig. 7.3(a), with perfect dispersion compensation such that XPM-induced nonlinear

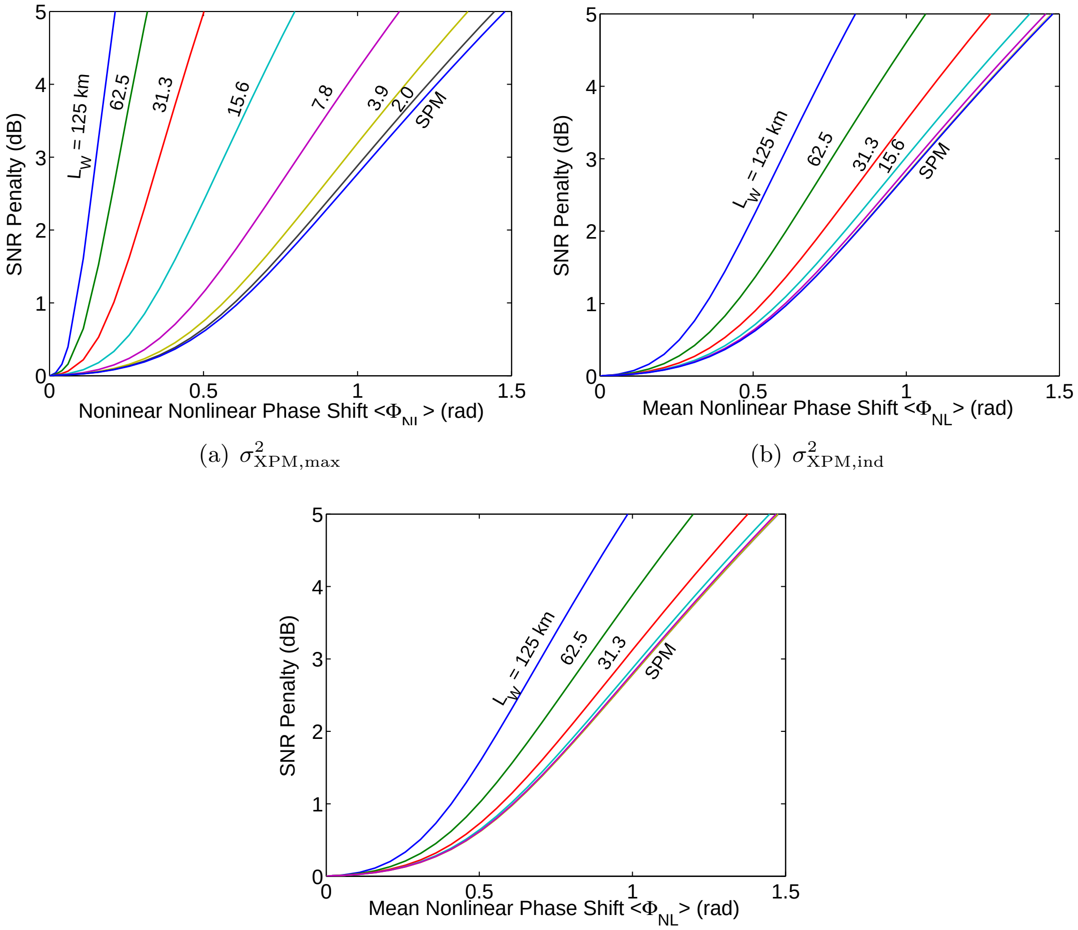

(a) $\sigma^2_{\mathrm{XPM,max}}$

(b) $\sigma^2_{\mathrm{XPM,ind}}$

(c) $\sigma^2_{\mathrm{XPM,min}}$

Figure 7.3: SNR penalty as a function of mean nonlinear phase shift $<\Phi_{\mathrm{NL}}>$ for WDM DPSK systems with various dispersion compensation schemes, corresponding to (a) maximum, (b) independent, and (c) minimum variance of XPM-induced nonlinear phase noise.

phase noise adds coherently, XPM-induced nonlinear phase noise gives the same SNR penalty as SPM-induced nonlinear phase noise when the walk-off length is about $L_W = 7.8$ km for $<\Phi_{\rm NL}>$ less than 1 rad. For a 10-Gb/s WDM system in SSMF, the channel spacing must be larger than or equal to 100 GHz (or 0.8 nm). For a 10-Gb/s WDM system in NZDSF, the channel spacing must be larger than or equal to 400 GHz (or 3.2 nm). For a 10-Gb/s WDM system with typical channel spacing of 50 or 100 GHz, with perfect dispersion compensation, the effect of XPM-induced nonlinear phase noise is larger than that induced by SPM. For a 40-Gb/s WDM system in NZDSF, the channel spacing must be larger than or equal to 100 GHz. With channel spacing larger than 100 GHz, typical 40-Gb/s WDM systems have a SNR penalty from XPM-induced nonlinear phase noise about that from SPM.

For the systems in Figs. 7.3(b) and (c), with dispersion compensation factor of Eq. (7.16) or with XPM suppressor, XPM-induced nonlinear phase noise gives the same SNR penalty as SPM-induced nonlinear phase noise when the walk-off length is about $L_W = 62.5$ km. For a 10-Gb/s WDM system in SSMF, the channel spacing must be larger than or equal to 12.5 GHz (or 0.1 nm). For a 10-Gb/s WDM system in NZDSF, the channel spacing must be larger than or equal to 50 GHz (or 0.4 nm). For a 10-Gb/s WDM system with typical channel spacing of 50 or 100 GHz, the effect of XPM-induced nonlinear phase noise is much smaller than that induced by SPM. Typical 40-Gb/s WDM systems have a SNR penalty from XPM-induced nonlinear phase noise far less than that from SPM.

7.2.3 Discussion

In the derivation of Eq. (7.6), the term of $|E_2|^2$ is ignored. For an non-return-to-zero (NRZ) DPSK signal, $|E_2|^2$ is a dc-term and can be ignored. For the more popular return-to-zero (RZ) DPSK signal (Gnauck et al., 2002, Zhu et al., 2003), $|E_2|^2$ is a periodic function with a period of T and its power spectral density is tones at k/T where k is integer. The differential transfer function of $2\sin^2(\pi f T)$ has notches at k/T and cancels all nonlinear phase noise due to $|E_2|^2$ even for RZ signal. For RZ-DPSK signal with pulse broadening due to fiber dispersion, if the dispersion is assumed to be a linear effect, for system without pulse overlapping, the differential transfer function can also completely eliminate XPM-induced nonlinear phase noise. Due to interferometer phase error (Ho, 2004, Kim and Winzer, 2003, Winzer and Kim, 2003), small residual nonlinear phase noise may be induced by those tones. The numerical results of this paper are also valid for flat-top RZ DPSK signals by increase the mean nonlinear phase shift by a factor equal to the inverse of the RZ pulse duty-cycle.

For the same channel spacing and fiber type, 10-Gb/s systems have a walk-off length four times that of 40-Gb/s systems. From Figs. 7.3, with the same mean nonlinear phase shift, the nonlinear phase noise induced SNR penalty of 10-Gb/s systems is smaller than that for the corresponding 40-Gb/s systems. However, 40-Gb/s systems have four times the bandwidth and require four times the power of the corresponding 10-Gb/s systems having the same SNR ρ_s defined in (Ho, 2003a,b). Because the mean nonlinear phase shift is proportional to the launched power, for the same SNR and system configuration, the mean nonlinear phase shift of 40-Gb/s systems is four times larger than that for 10-Gb/s systems.

When the dependence between nonlinear phase noise and amplifier noise is taking into account, we derive the exact error probability of DPSK signals with nonlinear phase noise when the number of fiber spans approaches infinity (Ho, 2003d). With the distributed assumption, the difference between exact and approximate error probability is less than 0.23 dB in term of SNR penalty. Currently, the exact error probability of DPSK signals with finite number of fiber spans is not known. From the simulation of (Ho, 2003a), the model of Eq. (7.18) is very accurate.

SPM-induced nonlinear phase noise correlates with the received intensity and can be compensated using the correlation properties (Ho, 2003a,d, Ho and Kahn, 2004, Liu et al., 2002, Xu and Liu, 2002). Other than using simultaneous multi-channel detection, XPM-induced nonlinear phase noise cannot be compensated.

Due to fiber dispersion, phase-modulation (PM) converts to amplitude-modulation (AM) noise. Combined with XPM, AM noise gives nonlinear phase noise to other channels (Norimatsu and Iwashita, 1993). When phase-modulation converts to amplitude-modulation, only high frequency AM noise is induced by a transfer function of $\sin(\alpha f^2)$, where α is a constant depending on fiber length and dispersion (Wang and Petermann, 1992). With the low-pass characteristic of $H_{12}(f)$ of Eq. (7.4), the combined effects of AM-PM conversion with XPM should be small.

7.2.4 Summary

Closed-form formulas are derived for the error probability of WDM DPSK signals contaminated by both SPM- and XPM-induced nonlinear phase noise. The error probability is derived based on the assumption that the phase of amplifier noise is independent of nonlinear phase noise. While SPM-induced nonlinear phase noise is not Gaussian-distributed, XPM-induced nonlinear phase noise is assumed to be Gaussian-distributed when either the walk-off length is small or number of WDM channels is large.

When fiber dispersion is compensated perfectly in each fiber span, XPM-induced nonlinear phase is summed coherently span after span and is the dominant nonlinear phase noise for typical multi-span WDM DPSK systems. For system without dispersion compensation or with XPM suppressor, the dominant nonlinear phase noise is typically induced by SPM. In general, with longer walk-off length, 10-Gb/s systems are more likely to be dominated by XPM-induced nonlinear phase noise than 40-Gb/s systems.

7.3 Other Degradation

Bibliography

Bellotti, G. and Bigo, S. (2000). Cross-phase modulation suppressor for multispan dispersion-managed WDM transmissions. *IEEE Photon. Technol. Lett.*, 12(6):726–728.

Bellotti, G., Bigo, S., Cortes, P.-Y., Gauchard, S., and LaRochelle, S. (2000). 10 × 10 Gb/s cross-phase modulation suppressor for multispan transmissions using WDM narrow-band fiber Bragg gratings. *IEEE Photon. Technol. Lett.*, 12(10):1403–1405.

Blachman, N. M. (1981). The effect of phase error on DPSK error probability. *IEEE Trans. Commun.*, COM-29(3):364–465.

Chiang, T.-K., Kagi, N., Fong, T. K., Marhic, M. E., and Kazovsky, L. G. (1994). Cross-phase modulation in dispersive fibers: theoretical and experimental investigation of the impact of modulation frequency. *IEEE Photon. Technol. Lett.*, 6(6):733–736.

Chiang, T.-K., Kagi, N., Marhic, M. E., and Kazovsky, L. G. (1996). Cross-phase modulation in fiber links with multiple optical amplifiers and dispersion compensators. *J. Lightwave Technol.*, 14(3):249–260.

Forghieri, F., Tkach, R. W., and Chraplyvy, A. R. (1995). Effect of modulation statistics on Raman crosstalk in WDM systems. *IEEE Photon. Technol. Lett.*, 7(1):101–103.

Forghieri, F., Tkach, R. W., and Chraplyvy, A. R. (1997). Fiber nonlinearities and their impact on transmission systems. In Kaminow, I. P. and Koch, T. L., editors, *Optical Fiber Telecommunications*, volume IIIA, pages 196–264. Academic Press, San Diego, CA.

Gnauck, A. H., Raybon, G., Chandrasekhar, S., Leuthold, J., Doerr, C., Stulz, L., Agrawal, A., Banerjee, S., Grosz, D., Hunsche, S., Kung, A., Marhelyuk, A., Maymar, D., Movassaghi, M., Liu, X., Xu, C., Wei, X., and Gill, D. M. (2002). 2.5 Tb/s (64 × 42.7 Gb/s) transmission over 40 × 100 km NZDSF using RZ-DPSK format and all-Raman-amplified spans. In *Optical Fiber Commun. Conf.* Optical Society of America, Washington, D.C. postdeadline paper FC2.

Gnauck, A. H., Raybon, G., Chandrasekhar, S., Leuthold, J., Doerr, C., Stulz, L., and Burrows, E. (2003). 25 40-Gb/s copolarized DPSK transmission over 12 100-km NZDF with 50-GHz channel spacing. *IEEE Photon. Technol. Lett.*, 15(3):467–469.

Gordon, J. P. and Mollenauer, L. F. (1990). Phase noise in photonic communications systems using linear amplifiers. *Opt. Lett.*, 15(23):1351–1353.

Gradshteyn, I. S. and Ryzhik, I. M. (1980). *Table of Integrals, Series, and Products*. Academic Press, San Diego.

Ho, K.-P. (2000). Statistical properties of simulated Raman crosstalk in WDM systems. *J. Lightwave Technol.*, 18(7):915–921.

Ho, K.-P. (2003a). Compensation improvement of DPSK signal with nonlinear phase noise. *IEEE Photon. Technol. Lett.*, 15(9):1216–1218.

Ho, K.-P. (2003b). Performance degradation of phase-modulated systems with nonlinear phase noise. *IEEE Photon. Technol. Lett.*, 15(9):1213–1215.

Ho, K.-P. (2003c). Probability density of nonlinear phase noise. *J. Opt. Soc. Amer. B*, 20(9):1875–1879.

Ho, K.-P. (2003d). Statistical properties of nonlinear phase noise. In Arkin, W. T., editor, *Advances in Optics and Laser Research*, volume 3, pages 1–2. Nova Science Publishers, Hauppauge, NY.

Ho, K.-P. (2004). The effect of interferometer phase error on direct-detection DPSK and DQPSK signals. *IEEE Photon. Technol. Lett.*, 16(1):308–310.

Ho, K.-P. and Kahn, J. M. (2004). Electronic compensation technique to mitigate nonlinear phase noise. *J. Lightwave Technol.*, 22(3):779–783.

Ho, K.-P., Kong, E. T.-P., Chan, L. Y., Chan, L.-K., and Tong, F. (1999). Analysis and measurement of root-mean-squared bandwidth of cross-phase-modulation-induced spectral broadening. *IEEE Photon. Technol. Lett.*, 11(9):1126–1128.

Jacobsen, G. and Garrett, I. (1987). Theory for optical heterodyne DPSK receivers with post-detection filtering. *J. Lightwave Technol.*, 5(4):478–484.

Jain, P. C. (1974). Error probabilities in binary angle modulation. *IEEE Trans. Info. Theory*, IT-20(1):36–42.

Kim, H. (2003). Cross-phase-modulation-induced nonlinear phase noise in WDM direct-detection DPSK systems. *J. Lightwave Technol.*, 21(8):1770–1774.

Kim, H. and Winzer, P. J. (2003). Robustness to laser frequency offset in direct-detection DPSK and DQPSK systems. *J. Lightwave Technol.*, 21(9):1887–1891.

Leibrich, J., Wree, C., and Rosenkranz, W. (2002). CF-RZ-DPSK for suppression of XPM on dispersion-managed long-haul optical WDM transmission on standard single-mode fiber. *IEEE Photon. Technol. Lett.*, 14(2):215–217.

Liu, X., Wei, X., Slusher, R. E., and McKinstrie, C. J. (2002). Improving transmission performance in differential phase-shift-keyed systems by use of lumped nonlinear phase-shift compensation. *Opt. Lett.*, 27(18):1616–1618.

Nelson, L. E., Jopson, R. M., Gnauck, A. H., and Chraplyvy, A. R. (1999). Resonances in cross-phase modulation impairment in wavelength-division-multiplexed lightwave transmission. *IEEE Photon. Technol. Lett.*, 11(7):907–909.

Nicholson, G. (1984). Probability of error for optical heterodyne DPSK system with quantum phase noise. *Electron. Lett.*, 20(24):1005–1007.

Norimatsu, S. and Iwashita, K. (1993). The influence of cross-phase modulation on optical FDM PSK homodyne transmission systems. *J. Lightwave Technol.*, 11(5):795–804.

Papoulis, A. (1984). *Probability, Random Variables, and Stochastic Processes.* McGraw Hill, New York, second edition.

Wang, J. and Petermann, K. (1992). Small signal analysis for dispersive optical fiber communication systems. *J. Lightwave Technol.*, 10(1):96–100.

Winzer, P. J. and Kim, H. (2003). Degradations in balanced DPSK receivers. *IEEE Photon. Technol. Lett.*, 15(9):1282–1284.

Xu, C. and Liu, X. (2002). Postnonlinearity compensation with data-driven phase modulators in phase-shift keying transmission. *Opt. Lett.*, 27(18):1619–1621.

Zhu, B., Nelson, L. E., Stulz, S., Gnauck, A. H., Doerr, C., Leuthold, J., Grüner-Nielsen, L., Pederson, M. O., Kim, J., Lingle, R., Emori, Y., Ohki, Y., Tsukiji, N., Oguri, A., and Namiki, S. (2003). 6.4-Tb/s (160 × 42.7 Gb/s) transmission with 0.8 bit/s/Hz spectral efficiency over 32 × 100 km of fiber using CSRZ-DPSK format. In *Optical Fiber Commun. Conf.* Optical Society of America, Washington, DC. postdeadline paper PD19.